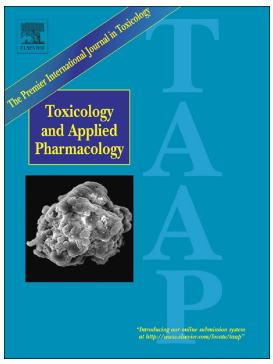

Induction of ABCG2/BCRP restricts the distribution of zidovudine to the fetal brain in rats

María Fernanda Filia, Timoteo Marchini, Juan Mauricio Minoia, Martín Ignacio Roma, Fernanda Teresa De Fino, Modesto Carlos Rubio, Guillermo J. Copello, Pablo A. Evelson, Roxana Noemí Peroni

PII: S0041-008X(17)30285-5
DOI: doi: 10.1016/j.taap.2017.07.005
Reference: YTAAP 14002

To appear in: *Toxicology and Applied Pharmacology*

Received date: 25 November 2016
Revised date: 21 June 2017
Accepted date: 6 July 2017

Please cite this article as: María Fernanda Filia, Timoteo Marchini, Juan Mauricio Minoia, Martín Ignacio Roma, Fernanda Teresa De Fino, Modesto Carlos Rubio, Guillermo J. Copello, Pablo A. Evelson, Roxana Noemí Peroni , Induction of ABCG2/BCRP restricts the distribution of zidovudine to the fetal brain in rats. The address for the corresponding author was captured as affiliation for all authors. Please check if appropriate. Ytaap(2017), doi: 10.1016/j.taap.2017.07.005

Induction of ABCG2/BCRP restricts the distribution of zidovudine to the fetal brain in rats

María Fernanda Filia[a], Timoteo Marchini[b#], Juan Mauricio Minoia[a], Martín Ignacio Roma[a], Fernanda Teresa De Fino[a], Modesto Carlos Rubio[a], Guillermo J. Copello[c], Pablo A. Evelson[b], Roxana Noemí Peroni[a*]

[a]*Instituto de Investigaciones Farmacológicas (ININFA UBA-CONICET), Facultad de Farmacia y Bioquímica, Universidad de Buenos Aires, Junín 956 5°, 1113, Ciudad Autónoma de Buenos Aires, Argentina.*

[b]*Universidad de Buenos Aires. CONICET. Instituto de Bioquímica y Medicina Molecular (IBIMOL), Facultad de Farmacia y Bioquímica, Cátedra de Química General e Inorgánica. Junín 956 2°, 1113, Ciudad Autónoma de Buenos Aires, Argentina.*

[c]*Cátedra de Química Analítica Instrumental e Instituto de Química y Metabolismo del Fármaco (IQUIMEFA UBA-CONICET), Facultad de Farmacia y Bioquímica, Universidad de Buenos Aires, Junín 956 5°, 1113, Ciudad Autónoma de Buenos Aires, Argentina*

#: both authors contributed equally to this manuscript

*Author for correspondence/Corresponding author:

Dra. Roxana N. Peroni

Instituto de Investigaciones Farmacológicas (ININFA UBA-CONICET), Facultad de Farmacia y Bioquímica, Universidad de Buenos Aires, Junín 956 5°, 1113, Ciudad Autónoma de Buenos Aires, Argentina

(54)-11-5287-4526, e-mail: rperoni@ffyb.uba.ar

Abstract

Safety concerns for fetus development of zidovudine (AZT) administration as prophylaxis of vertical transmission of HIV persist. We evaluated the participation of the ATP-binding cassette efflux transporter ABCG2 in the penetration of AZT into the fetal brain and the relevance for drug safety. Oral daily doses of AZT (60 mg/kg body weight) or its vehicle were administered between post gestational days 11 (E11) and 20 (E20) to Sprague-Dawley pregnant rats. At E21, animals received an intravenous bolus of 60 mg AZT/kg body weight in the presence or absence of the ABCG2 inhibitor gefitinib (20 mg/kg body weight, ip) and AZT in maternal plasma and fetal brain were measured by HPLC-UV. ABCG2 protein expression in placenta and fetal brain, as well as mitochondrial function and ultrastructure in fetal brain were also analyzed. *In utero* chronic exposure to AZT markedly induced ABCG2 expression in placenta and fetal brain whereas did not significantly alter mitochondrial functionality in the fetal brain. The area-under-the-concentration-time-curve of AZT significantly decreased in fetal brains isolated from AZT-exposed fetuses compared to control group, but this effect was abolished by ABCG2 inhibition. Our results suggest that the absence of mitochondrial toxicity in the fetal brain after chronic *in utero* administration of AZT could be attributed to its low accumulation in the tissue caused, at least in part, by ABCG2 overexpression. We propose that any interference with ABCG2 activity due to genetic, pathological or iatrogenic factors would increase the amount of AZT reaching the fetal brain, which could increase the risk of toxicity of this drug on the tissue.

Keywords: HIV; ABCG2; zidovudine; bioavailability; placenta; fetal brain

Introduction

The nucleoside analog reverse transcriptase inhibitor (NRTI) zidovudine (AZT) continues to play a key role as a drug for the prevention of maternal-fetal transmission of HIV. Prophylactic administration of AZT in combination with a second NRTI and a viral protease inhibitor reduces the mother-to-child HIV transmission to 1–2% in developed countries (HIV/AIDS, 2013). Unfortunately, exposure to AZT *in utero* encompasses the risk of long term mitochondrial-related toxicity that might be linked to hematological and cardiac tissue alteration in children (Barret et al., 2003; European Collaborative Study, 2004; Pacheco et al., 2006; Sibiude et al., 2015).

Transplacental kinetics of drugs are frequently mediated by ATP-binding cassette (ABC) efflux transporters embedded in the maternal face of the placenta (Staud et al., 2012). P-glycoprotein (ABCB1), multidrug resistance-associated protein 2 and 5 (ABCC2, ABCC5), and breast cancer resistance protein (ABCG2) are well-described placental transporters affecting the passage of their substrates into the fetal circulation (Ceckova-Novotna et al., 2006; Hahnova-Cygalova et al., 2011; Meyer zu Schwabedissen et al. 2005a; 2005b). In fact, a recent work reported in an *in situ* model of dually perfused rat placenta showed that ABCG2, and at lesser extent ABCB1, could be relevant for the passage of AZT from fetal to maternal side (Neumanova et al., 2015). Even though fetal-to-maternal plasma ratio of AZT is high (0.63-1.0) in Rhesus macaques and rats (Brown et al., 2003; Patterson et al., 1997), the transplacental passage of AZT markedly decreases whether AZT is co-administered with a BCRP substrate as acyclovir (Brown et al., 2003). Furthermore, it has been observed in Rhesus macaques that the accumulation of AZT is lower in fetal tissues

expressing ABC transporters from early stages of morphogenesis, such as the brain (Saunders et al., 2013, 2012), compared to other fetal organs (Patterson et al., 1997). In fact, the central nervous system displays a relative resistance to nucleoside analogs such as AZT, in both treatment and toxicity when compared to other organ systems even considering that the developing brain is particularly sensitive to mitochondrial damage (McCann et al., 2012). In support of a possible participation of ABCG2 in this phenomenon, experimental evidence has pointed out that this transporter is expressed at higher levels and is functionally more active in the developing than in the adult brain (Ek et al., 2012). Additionally, ABCG2 expression has also been found in the fetal brain endothelium as early as post-gestational day 12 (E12) in rats (Kalabis et al., 2007).

Moreover, it was shown that the efflux of antiretroviral drugs by ABCG2 seems to become of relevance whether a high density of molecules are present in the cell membrane, as occurred either in transfected or transformed cell lines (Pan et al., 2007; Wang et al., 2004, 2003; Weiss et al., 2007) or under *in vivo* repeated exposure to a substrate as efavirenz (Peroni et al., 2011; Roma et al., 2015).

We propose that the low incidence of neurological damage associated with mitochondrial dysfunction in children exposed *in utero* to AZT (Ek et al., 2010) could be related, at least in part, to the restriction of AZT passage across both the placenta and the developing blood-brain barrier by induction of ABCG2. The aim of this study was to analyze whether ABCG2 restricts the accumulation of AZT in fetal brain after chronic *in utero* exposure in pregnant rats protecting against mitochondrial toxicity. We developed a model of chronic

AZT administration leading to overexpression of ABCG2 in placenta and fetal brain that induced the efflux of AZT out of the fetal brain.

1. Materials and methods

1.1. Materials

AZT was provided by Laboratorios Richmond (Buenos Aires, Argentina). Gefitinib was obtained from Astra-Zeneca (Chesire, UK). Protease inhibitor cocktail (Complete mini, Roche Applied Science, Mannheim, Germany) and phenylmethylsulfonyl fluoride (PMSF, Sigma-Aldrich, St. Louis, MO) and every other chemical not listed here were of the highest purity available and were used as received.

1.2. Methods

1.2.1. Animals and treatments

Female Sprague-Dawley rats (8 weeks, 150-200 g body weight) were housed under a 12:12-h light:dark cycle, at controlled room temperature with food and water *ad libitum*. All procedures involving animals were conducted in accordance with NIH guidelines for the Care and Use of Laboratory Animals (Institutional Animal Care and Use Committee Guidebook, 2nd ed., 2002). The 3Rs principle of Reduction, Refinement, and Replacement was considered in the design of the animal experiment and applied when possible. Animal treatment was carried out in accordance with the guidelines of the 6344/96 regulation of the Argentinean National Drug, Food and Medical Technology Administration (ANMAT).

Pregnancy was confirmed by the presence of sperm in the vaginal smear the morning after matting and was considered post gestational day 0 (E0). Control pregnant rats at E11, E13,

E15, E18 or E21 (n=3 per group) were used in this study. The day of the assay, rats were anaesthetized with 1.2 g/kg urethane (i.p.) and subsequent doses of anesthesia were administered as needed. A laparotomy was performed and a small incision was made in the uterine wall to allow for sampling of the pups.

Treatments: Twenty-four pregnant rats were randomly divided into two groups, given either 60 mg / kg body weight zidovudine (AZT) or vehicle (0.05% ethanol in saline solution) from E11 to E20 orally by esophageal catheter. In E21, the animals from each group were again divided into two subgroups for the administration of the selective inhibitor of ABCG2 gefitinib (GFT, 20 mg/kg) or vehicle (dimethyl sulfoxide:propylene glycol:saline solution, in a 2:2:1 ratio), respectively, 30 min before the onset of pharmacokinetic assays. In this way, 4 groups were constituted: VEH / VEH, AZT / VEH, VEH / GFT, and AZT / GFT (n = 6 per group).

2.2.3. ABCG2 protein expression levels and localization

2.2.3.1. Western Blot in placenta and fetal brain

Placenta (at E11, E15, E18, and E21) and fetal brain (E18 and E21) were collected from pregnant rats within 30 min of surgery and immediately stored at -70° C. To prepare samples for western blotting analysis, total protein was obtained from tissues defrosted on ice and measured with bovine serum albumin (BSA, A7906 Sigma-Aldrich, USA) as standard (Lowry et al., 1951) and analyzed as previously described (Peroni et al., 2011). Briefly, placenta from E11 and E15 (pool of three, 30 µg of protein per line), E18 and E21 (30 µg of protein per line), and fetal brain from E18 and E21 (pool of three; 50 µg of protein per line) were loaded onto 8 % SDS-polyacrylamide gels, subjected to electrophoresis and transferred to nitrocellulose membranes. After blocking, membranes

were cut at molecular mass 52 kDa, based on the Kaleidoscope molecular weight standards (Bio-Rad, Hercules, CA, USA). The upper and lower portions were then incubated overnight at 4° C with anti-rat ABCG2 antibody (M-70, 1:400; Santa Cruz Biotechnology, Santa Cruz, CA, USA) or mouse anti-ABCG2 antibody (BXP-21 clone 1/400, Santa Cruz Biotechnology, CA, USA, SC-58222) and anti-actin antibody (A2066, 1:1000; Sigma-Aldrich, USA), respectively. The immune complex was detected by incubation with the horseradish peroxidase-linked anti-rabbit antibody (sc-2004, 1/2000; from Santa Cruz Biotechnologies) or horseradish peroxidase-linked goat anti-mouse IgG (sc-2031, 1/2000; from Santa Cruz Biotechnologies) during 90 min. The bands were detected by chemiluminescence (Amersham ECL Biosciences, Amersham, UK) and quantified by densitometric analysis using ImageJ software (1.34S, US National Institutes of Health, Bethesda, MD, USA).

2.2.3.2. Immunofluorescence in fetal brain tissue

Fetus obtained by cesarean surgery on E21 were decapitated and the brain were carefully removed from skull, washed in cold 0.1 M K_2HPO_4/KH_2PO4, pH 7.4 (PB), placed in a pre-chilled glass platen, and cleaned to remove meninges and choroid plexus. One hemisphere of each brain was postfixed in 4% paraformaldehyde / PB at 4 °C for 24 h, cryoprotected overnight in 30% sucrose/PB. Four serial hemi-coronal slices (20-µm thickness) at 3 mm (striatal level) from the frontal tip were performed with a rotary microtome cryostat (Thermo Scientific), mounted in gelatinized glass slides and stored at −20°C until use. Two section of each series was stained with hematoxylin and eosin (H&E) according to standard protocols and observed at under low as well as 200 × magnification. For immunofluorescence, another two section of each series were blocked with 5% fetal calf

serum (FCS) in phosphate saline buffer (PBS) for 1 h prior incubation with mouse anti-ABCG2 antibody (BXP-21 clone 1/100, Santa Cruz Biotechnology, SC-58222) overnight at 4 °C. The BXP-21 antibody clone has previously been shown to specifically react with a 72 kDa protein in rat fetal brain (Ek et al., 2010). Slides were incubated with goat anti-mouse IgG (Fc specific)–biotin antibody (1/250 Sigma Aldrich, B7401) overnight at 4 °C, followed by 1 h incubation with DTAF-streptavidin (1/500 Jackson ImmunoResearch Laboratories Inc, TechFAQ #6) at room temperature. All antibodies were diluted in 3% FCS/0.3% Tween20 PBS and three washes with 0.3%-Tween20 PBS were performed between each step. Tissues were mounted with Mowiol and coverslipped. Control sections omitting primary antibody were prepared in each slide and were always blank. Photographs were taken with an optical microscope (Nikon Eclipse) equipped with fluorescent optics and a camera connected to a monitor and computer. Digital images were color balanced with Adobe Photoshop 8.0 (Adobe Systems). The average intensity value of each particle was background subtracted using the average intensity of an adjacent region of comparable size.

2.2.4. Mitochondrial function and structure

2.2.4.1. Isolation and preparation of mitochondrial membranes

Mitochondrial purified fractions from fresh fetal brain homogenates isolated from E21 pups treated with AZT or its vehicle (n=4 per group) were obtained by differential centrifugation in a Sorvall RC5C centrifuge (Sorvall, Buckinghamshire, England). Five fetal brains were pooled, washed, and minced in ice-cold STE buffer [250 mM sucrose, 5 mM Tris-HCl, and 2 mM EGTA (pH 7.4)]. Samples were homogenized in 1:10 STE buffer and centrifuged at 700g for 10 min. The sediment was discarded and mitochondria were pelleted from the

supernatant by a second centrifugation step at 8000g for 10 min. Finally, the pellet was washed, rinsed, and resuspended in 500 µL of STE buffer. The whole procedure was carried out at 0-4 °C (Mela and Seitz, 1979). Mitochondrial membranes were obtained by three freeze-thaw cycles of the mitochondrial preparation, followed by a homogenization step by passage through a 29G hypodermic needle (Boveris et al., 2002).

2.2.4.2 Mitochondrial respiration

Mitochondrial oxygen consumption was assessed by polarography using a Clark-type oxygen electrode (Hansatech Oxygraph, Hansatech Instruments Ltd, Norfolk, England) for high resolution respirometry at 30 °C. Freshly isolated brain mitochondria (1 mg protein/mL, n=4 per group) were incubated in respiration buffer [120 mM KCl, 5 mM KH_2PO_4, 1 mM EGTA, 3 mM HEPES, and 1 mg/mL fatty acid-free BSA (pH 7.2)] supplemented with 2 mM malate and 5 mM glutamate, or 8 mM succinate. An initial rest state respiration (state 4) was established under these conditions, which was then switched to active state respiration (state 3) by the addition of 1 mM ADP. Respiratory control ratio (RCR) was calculated as state 3/state 4 respiration rates. Results were expressed as ng-at O/min mg protein (Boveris et al., 1999).

2.2.4.3. Mitochondrial respiratory chain complexes activity

The enzymatic activity of mitochondrial respiratory complexes was evaluated by a colorimetric assay in a Beckman DU 7400 diode array spectrophotometer (Beckman Coulter Inc., CA, USA). Mitochondrial membranes (0.25 mg protein/mL) were incubated at 30 °C in 100 mM PBS (pH 7.2). For complexes I and II, reaction x was supplemented with 0.2 mM NADH or 5 mM succinate as substrates, respectively, plus 25 µM cytochrome c^{3+}

and 0.5 mM KCN. Cytochrome c^{3+} reduction rate was followed at 550 nm (ε = 19 mM^{-1} cm^{-1}) and results were expressed as nmol reduced cytochrome c^{3+}/min mg protein. For complex IV, reaction buffer was instead supplemented with 60 µM cytochrome c^{2+}. In this case, cytochrome c^{2+} oxidation rate was calculated from the pseudo-first reaction constant (k´) and expressed as k´/mg protein (Yonetani, 1967).

2.2.4.4. Mitochondrial membrane potential

Freshly isolated brain mitochondria (25 µg protein/mL, n=4 per group) were incubated with the potentiometric cationic probe 3,3′-dihexyloxacarbocyanine iodide ($DiOC_6$) (30 nM) in respiration buffer. The procedure was performed in the dark at 37 °C for 20 min. After the incubation period, mitochondria were acquired in a FACSCalibur flow cytometer (BD Biosciences, San Jose, CA, USA). To exclude debris, samples were gated based on light-scattering properties and 20,000 events per sample within this gate were collected. 10-N-nonyl acridine orange (NAO) (100 nM) was used to selectively stain mitochondria and to evaluate their purity, due to its ability to selectively bind to cardiolipin at the inner mitochondrial membrane (Haines and Dencher, 2002). Samples were analyzed in the FL-1 channel with FlowJo software (Tree Star, Ashland, OR, USA), and the arithmetic mean values of the median fluorescence intensities (MFI) were obtained. Autofluorescence (negative control) was evaluated in isolated brain mitochondrial samples without $DiOC_6$. Total depolarization induced by carbonyl cyanide m-chlorophenyl hydrazine (m-CCCP) (2 µM) was used as a positive control. Mitochondrial preparations that showed no changes in membrane potential under this condition were discarded (Marchini et al., 2013).

2.2.4.5. Ultrastructural analysis of fetal brain mitochondria

2.2.4.5.1. Tissue preparation for transmission electron microscopy

Fetus removed by cesarean surgery on E21 were decapitated and brains were carefully removed, washed in chilled PB and placed in a pre-chilled glass platen. Four pieces of 1-2 mm^3 were obtained from four different areas of the cerebral cortex and fixed with 2.5% glutaraldehyde/PB for 4 h. Samples were postfixed in 1% osmium tetroxide/PB for 1.5 h at 0 °C. Samples were contrasted with 5% uranyl acetate for 2 h at 0 °C, dehydrated, and embedded in Durcupan resin (Fluka AG, Switzerland) for 72 h at 60 °C. Ultrathin sections were cut and observed with a Zeiss EM 109 transmission electron microscope (Oberkochen, Germany). Representative digital images were captured using a CCD GATAN ES1000W camera (CA, USA).

2.2.4.5.2. Electron microscopic evaluation

Random sections were selected for analysis by an electron microscopy technician blinded to the treatments. Using the "point counting grids" methodology (Vanasco et al., 2014), mitochondrial density was determined. For each sample, 10 photomicrographs at 85,000X, were evaluated for mitochondrial morphology. The degree of mitochondrial pathology was scored by two different investigators, all of whom were given coded photomicrographs to eliminate bias. Scoring paradigm for mitochondrial status in brain cortex is detailed in legend at Figure 3.

2.2.5. Thiobarbituric acid reactive substances (TBARS) assay in fetal brain homogenate

The TBARS assay is the classical approach in order to evaluate the extent of lipid peroxidation processes in biological samples (Yagi, 1976). Briefly, 100 µL of brain homogenates were mixed with 200 µL 0.1 N HCl, 30 µL 10% (w/v) phosphotungstic acid and 100 µL 0.7% (w/v) 2-thiobarbituric acid, and incubated at 95 °C for 60 min. Afterwards, samples were cooled and TBARS were extracted in 1 mL of n-butanol. After a 10 min centrifugation at 800 g, the fluorescence of the butanol layer was measured in a Perkin Elmer LS 55 luminescence spectrometer (Perkin Elmer, MA, USA) at 515 nm (excitation) and 553 nm (emission). A calibration curve was prepared using 1,1,3,3-tetramethoxypropane as standard. Results were expressed as nmol TBARS/mg protein.

2.2.6. Pharmacokinetic analysis

2.2.6.1. Sample collection

For pharmacokinetic assays, rats were anaesthetized with urethane (1.2 g/kg, i.p and supplemented to loss of reflexes). Prior to dosing, a laparotomy was performed and a small incision was made in the uterine wall to allow for sampling of the pups, and cannulas were surgically implanted in the right femoral vein and in the carotid artery

The pharmacokinetic study consisted of an intravenous administration through the femoral vein of 60 mg / kg AZT (0.05% ethanol in saline solution) and its concentration in maternal blood and fetal brain was determined at times 0, 1, 2, 5, 10, 15, and 30 min. The dose was selected on the basis of a previous study that shows quantifiable values of AZT in placenta, amniotic fluid as well as in total fetal tissue homogenates (Brown et al., 2003). For each point, 150 µl of heparinized maternal blood was collected by carotid artery and 1 fetal sac. Body temperature was maintained by heated surgical pads and incandescent lights. The blood supply to the individual fetus was tied off prior to removal to minimize bleeding.

Blood was placed into heparinized tubes. Fetal brains were isolated from the pups and homogenized in 2 volumes of deionized water (wt/vol). Proteins were precipitated by addition of 15% trichloroacetic acid on ice for 15 min with vortex and then centrifuged 10 min at 5000g. Supernatants were stored at 70°C until analysis.

2.2.6.2. Quantification of AZT in biological samples: Instrumentation: The HPLC system consisted in a Spectra series P100 pump (Thermo separation products, Virginia, USA), with a 20 µL injection loop. Separation was performed using a Luna C8 column (250 X 4.6 mm, 5 µm particle size, Phenomenex, CA, USA) for AZT samples.

Chromatographic conditions: Isocratic elution at room temperature; flow rate: 1.2 ml/min. UV Detection: 266 nm for AZT. Mobile phase: 20 mM sodium phosphate buffer (containing 8 mM 1-octanesulfonic acid sodium salt)–acetonitrile (86:14, v/ v) with pH adjusted to 3.2 with phosphoric acid (Fan and Stewart, 2002). Samples were injected in duplicate into the HPLC column.

Pharmacokinetics analysis: All data were analyzed using the freely available menu-driven add-in program for Microsoft Excel PK*solver* (Zhang et al., 2010). A non-compartamental analysis was performed for concentration-time profiles data and area under the curve of AZT from 0 to infinity (AUC $AZT_{0\rightarrow\infty}$) for each sample were extracted.

2.2.7. Statistical analyses

Data are presented as the mean ± S.E.M. (n = 4 to 6) analyzed with Graph Pad Prism 5 (Graph Pad Software). Pharmacokinetic assays were analyzed by two-way analysis of variance followed by Bonferroni's *ad hoc* post test. AUC and western blot assays were

analyzed by one-way analysis of variance followed by Bonferroni's multiple comparison test. TBARS assay, mitochondrial respiration, respiratory complexes activities, mitochondrial potential and mitochondrial ultrastructure were analyzed by Student t-test.

3. Results

3.1. Effect of AZT on the expression of ABCG2 in placenta and fetal brain

To validate our experimental model, a time course of ABCG2 protein expression in placenta was performed in control Sprague-Dawley rats from middle to term gestation covering the period in which the animals would be subsequently treated with AZT (E11 to E21). A band of approximately 72 kDa corresponding to the molecular weight of the monomer of ABCG2 was observed in placenta. As shown in Supplemental File 1A, ABCG2 showed maximal expression at E15 although the difference failed to reach statistical significance respect to E11. From E15 to hereinafter ABCG2 significantly decreased becoming almost undetectable in E21 (Supplemental File 1A and B). Moreover, a significant decreased in ABCG2 expression was also observed in fetal brains between E18 and E21 (Supplemental File 1A and B).

To evaluate the effect of chronic exposure to AZT, pregnant rats were treated with 60 mg/kg body weight AZT or its vehicle (0.05 % ethanol in saline solution) daily by gavage from E11 to E20. Expression of ABCG2 in the placenta and fetal brain of vehicle-treated animals was not significantly different from that found in control animals (Figure 1A and B). A significant induction of ABCG2 protein in both tissues was observed in rats chronically exposed to AZT compared to vehicle-treated animals (Fig. 1B). When we performed a histological analysis in fetal brain slices from both groups by the H&E technique, we observed that both the architecture and the number of cells at the level of the

developing striatum did not show differences between those tissues obtained from rats treated with vehicle compare with those treated with AZT (Fig. 1C and F). Immunofluorescence for ABCG2 performed in the same area of the brain showed a higher immunoreactivity for the protein in fetal brains isolated from rats chronically exposed to AZT (Fig. 1D) respect to vehicle-treated ones (Fig. 1 G). At higher magnification (Fig. 1E and H), it could be observed that immunoreactivity for ABCG2 in the fetal brain cortex was exclusively localized to blood vessels structures in accordance to that observed by Ek et al (Ek et al., 2010).

3.2. Effect of chronic oral administration of AZT in the functionality and ultrastructure of fetal brain mitochondria

Since AZT causes alterations in the mitochondrial energy-generating mechanism (Szewczyk and Wojtczak, 2002), we analyzed oxygen consumption in freshly isolated mitochondria from fetal brain. We did not observed modifications in the respiratory consumption ratio (RCR) using malate plus glutamate, or succinate, as respiratory substrates in brain mitochondria isolated from pups exposed *in utero* to AZT respect to the vehicle-treated ones (Table 1). In addition, as shown in Table 2, no changes were detected when the activity of the respiratory chain complexes I or II were assessed, whereas a slight but no significant increase in Complex IV was found in the AZT-exposed group.

Mitochondrial membrane potential comprises another key feature of mitochondrial function. Isolated brain mitochondria were selected from background based on light-scattering properties (SSC vs FSC, Fig. 2A) and gated events were chosen for analysis. In every analyzed preparation, >95% of gated events were NAO-positive compared with unstained control samples (Fig. 2B), indicating that contamination with other subcellular

constituents throughout the isolation procedure was kept at minimum. Moreover, no significant differences were observed in NAO MFI between control and AZT-exposed pups (Fig. 2C). Regarding mitochondrial membrane potential, as it is shown in $DiOC_6$ overlaid histograms (Fig. 2D) and quantification as MFI (Fig. 2E), no significant differences were also observed between control and AZT-exposed pups.

We also analyzed the mitochondrial ultrastructure of the fetal cerebral cortex in E21. Several parameters of mitochondrial damage were observed in tissues isolated from animals treated either with vehicles (Fig. 3A-E) or chronically exposed to AZT (Fig. 3F-J), such as those detailed in the legend of Figure 3. The results of mitochondrial damage score quantification, performed by two investigators on a total of 10 tissue photomicrographs at 85000x magnification (Fig. 3E and J) and in turn in duplicate, showed that there were no significant differences in the mitochondrial status of the cerebral cortex between the treated and vehicle groups (Fig. 3K).

3.3. Lipidic peroxidation in fetal brain homogenate

Another parameter of mitochondrial damage is the over production of reactive species of oxygen that leads to oxidative damage to lipids. Furthermore, in our experimental conditions, no significant changes in TBARS levels were observed in fetal brain homogenate of fetuses isolated from mothers treated with AZT respect to the animals receiving vehicle (Fig. 3L) precluding an over extent of lipid peroxidation processes.

3.4. Effect of chronic oral administration of AZT on its accumulation in the distribution to the fetal brain

In order to evaluate the passage of AZT to fetal brain in our model and the participation of ABCG2, we proceeded to administer an i.v. dose of 60 mg AZT/kg body weight in term-pregnancy rats chronically exposed to either the drug or the vehicle in control conditions of after a 30 min-pre administration of the selective inhibitor of ABCG2 gefitinib [20 mg/kg i.p.; (Roma et al., 2015)]. Drug levels were quantified in maternal blood as well as in fetal brain at different times by HPLC-UV. No detectable levels of AZT were found at time 0 in either maternal blood or fetal brain in samples obtained from animals chronically treated with AZT. No differences were found in the concentration-versus-time curves for AZT in maternal blood between vehicle groups and chronically exposed to AZT (Fig 4A), even in the presence of the inhibitor of ABCG2 gefitinib (Fig 4B). In addition, Figure 4C shows that inhibition of ABCG2 does not modify AZT levels in maternal blood, as no changes were observed in the corresponding area under the curve from 0 to infinite in maternal plasma ($AUC_{0\rightarrow\infty\ plasma}$; Fig. 4C).

Unlike what was observed in maternal plasma, Fig. 5A, the kinetic profile and the $AUC_{0\rightarrow\infty}$ of AZT in fetal brains from pups chronically exposed *in utero* to AZT was significantly reduced with respect to the vehicles in control conditions (Fig. 5A). Nevertheless, this difference disappeared after ABCG2 inhibition (Fig. 5B), which was also reflected in changes in the accumulated amount of drug in the tissue represented as the area under the curve ($AUC_{0\rightarrow\infty}$) in Fig. 5C, suggesting that induction of ABCG2 have a relevant participation in limiting the penetration of AZT in the fetal brain.

Moreover, the concentration of AZT in fetal brain and maternal blood showed no difference when analyzed in E11 (data not shown).

4. Discussion

The goal/aim of this study was to evaluate the *in vivo* contribution of the efflux transporter ABCG2 to the delivery of the substrate AZT towards the fetal brain using a model of chronic oral administration of the drug in pregnant rats. We have found that sustained exposure to AZT induced ABCG2 in placenta and fetal brain. Moreover, decreased accumulation of AZT in fetal brain, because of an efflux mechanism due to the induction of ABCG2, would account for the absence of mitochondrial toxicity that we found in this tissue. Our results are in accordance with the low prevalence of adverse neurologic effects compared to other organs, such as heart, muscle, and blood cells, in infants exposed to the NRTIs in utero (King, 2004). In this sense, it has been shown that high experimental AZT doses are required to cause neurologic abnormalities in fetuses chronically exposed to AZT (McCann et al., 2012).

ABC transporters collaborate with the elimination of lipophilic compounds that reach the fetal compartment (Figueroa et al., 2010; Löscher and Potschka, 2005). ABCG2 is highly expressed in placenta in several species (Maliepaard et al., 2001), but it undergoes substantial changes during normal placental development (Hahnova-Cygalova et al., 2011). From E11 to E21 in rats, that could be extrapolated to the time window in which AZT is recommended for the prophylaxis of vertical transmission of HIV in women, we found that placental ABCG2 gradually decreased to become almost undetectable near to parturition (Figure 1A, 1B). This is in agreement with previous works in rats, mice and humans (Wang et al., 2006; Yasuda et al., 2005). In turn, the present observation that ABCG2 in fetal brain decreased from E18 to E21 (supplemental file 1) is in accordance with previous reported evidences (Cygalova et al., 2008). Moreover, ABCG2 seems to localize to the blood-facing

side of epithelial cells of brain in early fetal stages at higher levels than in postnatal days giving additional neuroprotection to that provided by the placenta (Ek et al., 2010).

AZT disposition between mother and fetus have shown to be poorly modulated by ABCG2 when tested in rat term placenta (Neumanova et al., 2016) with almost undetectable levels of the transporter as previously reported (Mao, 2008) and in the present work (Figure 1). Even so, pharmacokinetics of AZT in near-term pregnant rats adjusted to a two-compartment model with first order elimination, but when it is co-administered with the ABCB1/ABCG2 substrate acyclovir (Gunness et al., 2011), an increased access of both drugs to fetal tissues is observed (Brown et al., 2003), suggesting that ABC transporters could act as fetal barriers mechanisms (Brown et al., 2003). Since AZT is both substrate and modulator of ABCG2 *in vitro* (Wang et al., 2004, 2003), it could be possible that in conditions coursing with higher levels of ABCG2, this transporter could restrict AZT disposition. In this sense, no histologic alterations, at least at striatal level, were found in fetal brains exposed in utero to AZT in our model (Fig 1 C and F). An induction of ABCG2 could be attained by sustained substrate exposure, as we previously observed for the overexpression of ABCG2 in small intestine and blood-brain barrier caused by efavirenz (Peroni et al., 2011; Roma et al., 2015) as well as in the placenta and in the fetal brain (present work, Fig 1A and 1B). Moreover, immunofluorescence showed that an specific mark for ABCG2 localized in blood vessels structures in the cortex fetal brain (Fig 1C-F; (Ek et al., 2010) confirms the presence of this transporter in the developing brain-barrier exerting efflux mechanisms.

The amount of AZT that can cross placenta and reaches fetal circulation is relevant for mitochondrial function. It was reported that AZT alters the enzymes involved in mitochondrial energy production by a short-term oxidative stress-mediated mechanism (Szabados et al., 1999) and affects mitochondrial proteins synthesis through long-term damage of mitochondrial DNA (Szewczyk and Wojtczak, 2002). In our model, *in utero* exposure to AZT during the second half of gestation did not cause alterations in mitochondrial function assessed through mitochondrial oxygen consumption, respiratory chain complexes activity, and inner membrane potential (Table 1, Table 2 and Figure 2). In addition, the absence of AZT exposure-related alterations of mitochondria ultrastructure in fetal brain found reported here (Fig 3A-K) is consistent with findings in primates exposed to AZT *in utero*, where mitochondrial brain compromise is observed only whether AZT is associated to other NRTIs perinatally (Divi et al., 2010; Gerschenson et al., 2000). The present findings that show preserved functionality and structure in mitochondria, are in agreement with previously published studies designed to examine neurodevelopment in infants born to HIV-1–infected mothers, since it has not been reported neurodevelopmental/cognitive compromise that is due only to HAART exposure (Alimenti et al., 2006). In turn, the absence of alterations in the lipidic peroxidation parameters in the brain tissue of fetuses exposed *in utero* to AZT with respect to the vehicles (Fig. 3L) is another present finding that reinforces the absence of fetal brain damage observed in our model and which may be related to low tissue exposure to the drug. Supporting this observation, is the present finding showing a marked decrease of AZT concentrations in fetal brain in chronic-exposed animals (Fig. 5) without changes in the levels of AZT in maternal blood (Fig 4). In accordance with this, a low penetration of the ABCG2 substrate cimetidine to the fetal brain was also reported (Cygalova et al., 2008). Furthermore, our

hypothesis that induction of ABCG2 restrict the access of AZT to fetal brain was confirmed by the significant increase (nearly 70 %) in AZT levels in fetal brains from chronically-treated drug pregnant rats, that equated those found in vehicles, when ABCG2 was inhibited by gefitinib (Fig 5B and 5C). Moreover, this increase in AZT levels in fetal brain occurred at the expense of an inhibition of ABCG2 at both the placenta and fetal brain since maternal blood concentrations remained unchanged, as demonstrated by increased $AUC_{fetal\ brain}$ /$AUC_{maternal\ blood}$ ratio (Fig. 5D). On the other hand, the absence of changes in the animals treated with vehicles could likely be due to the almost null expression of ABCG2 in the placenta and the fetal brain of these animals. Still, it is not excluded that there is another efflux transporter that regulates the AZT passage through the placenta or the blood-brain barrier.

The relevance of ABCG2 on AZT fetal disposition seems to be dependent on variables that affect the transporter expression levels or activity. Possible scenarios are the combination of AZT with either the ABCG2 inhibitor ritonavir (Bierman et al., 2010) or the ABCG2 substrates nitrofurantoin and sulfasalazine, which are commonly prescribed for pregnant women that have been shown to have ABCG2 activity-depending pharmacokinetics (Goldberg et al., 2015; Lee et al., 2015; Ni et al., 2010) as well as ABCG2 gene polymorphisms (Mao, 2008).

We consider that to be able/in order to minimize the risk of toxicity affecting newborns, it is of interest to understand all factors potentially affecting AZT disposition in fetus. , Co-administration of AZT with other ABCG2 substrates or inhibitors with narrow therapeutic range might interfere with ABCG2 activity due to genetic, pathological or iatrogenic

factors that would increase the amount of AZT reaching the fetal brain, increasing the risk of toxicity of this drug on target tissues.

Acknowledgements

The present work was fully sponsored by the National Research Council and the University of Buenos Aires from Argentina with grant numbers PIP 11220120100499 and 20020100100198, respectively. We are especially grateful to María Mercedes Odeón, Ph. D. and Gimena Gómez, Biochemist; for their valuable advice in conducting immunofluorescence assays and to Betina González, Ph. D. for her participation in the analysis of the mitochondrial ultrastructure.

5. Bibliography

Alimenti, A., Forbes, J.C., Oberlander, T.F., Money, D.M., Grunau, R.E., Papsdorf, M.P., Maan, E., Cole, L.J., Burdge, D.R., 2006. A Prospective Controlled Study of Neurodevelopment in HIV-Uninfected Children Exposed to Combination Antiretroviral Drugs in Pregnancy. Pediatrics 118, e1139–e1145.

Barret, B., Tardieu, M., Rustin, P., Lacroix, C., Chabrol, B., Desguerre, I., Dollfus, C., Mayaux, M.-J., Blanche, S., French Perinatal Cohort Study Group, 2003. Persistent mitochondrial dysfunction in HIV-1-exposed but uninfected infants: clinical screening in a large prospective cohort. AIDS 17, 1769–85.

Bierman, W.F.W., Scheffer, G.L., Schoonderwoerd, A., Jansen, G., van Agtmael, M.A.,

Danner, S.A., Scheper, R.J., 2010. Protease inhibitors atazanavir, lopinavir and ritonavir are potent blockers, but poor substrates, of ABC transporters in a broad panel of ABC transporter-overexpressing cell lines. J. Antimicrob. Chemother. 65, 1672–80.

Boveris, A., Arnaiz, S.L., Bustamante, J., Alvarez, S., Valdez, L., Boveris, A.D., Navarro, A., 2002. Pharmacological regulation of mitochondrial nitric oxide synthase. Methods Enzymol. 359, 328–39.

Boveris, A., Costa, L.E., Cadenas, E., Poderoso, J.J., 1999. Regulation of mitochondrial respiration by adenosine diphosphate, oxygen, and nitric oxide. Methods Enzymol. 301, 188–98.

Brown, S.D., Bartlett, M.G., White, C.A., 2003. Pharmacokinetics of intravenous acyclovir, zidovudine, and acyclovir-zidovudine in pregnant rats. Antimicrob. Agents Chemother. 47, 991–6.

Ceckova-Novotna, M., Pavek, P., Staud, F., 2006. P-glycoprotein in the placenta: expression, localization, regulation and function. Reprod. Toxicol. 22, 400–10.

Cygalova, L., Ceckova, M., Pavek, P., Staud, F., 2008. Role of breast cancer resistance protein (Bcrp/Abcg2) in fetal protection during gestation in rat. Toxicol. Lett. 178, 176–80.

Divi, R.L., Einem, T.L., Fletcher, S.L.L., Shockley, M.E., Kuo, M.M., St Claire, M.C., Cook, A., Nagashima, K., Harbaugh, S.W., Harbaugh, J.W., Poirier, M.C., 2010. Progressive mitochondrial compromise in brains and livers of primates exposed in utero to nucleoside reverse transcriptase inhibitors (NRTIs). Toxicol. Sci. 118, 191–201.

Ek, C.J., Dziegielewska, K.M., Habgood, M.D., Saunders, N.R., 2012. Barriers in the developing brain and Neurotoxicology. Neurotoxicology 33, 586–604.

Ek, C.J., Wong, A., Liddelow, S.A., Johansson, P.A., Dziegielewska, K.M., Saunders, N.R., 2010. Efflux mechanisms at the developing brain barriers: ABC-transporters in the fetal and postnatal rat. Toxicol. Lett. 197, 51–9.

European Collaborative Study, 2004. Levels and patterns of neutrophil cell counts over the first 8 years of life in children of HIV-1-infected mothers. AIDS 18, 2009–17.

Fan, B., Stewart, J.T., 2002. Determination of zidovudine/lamivudine/nevirapine in human plasma using ion-pair HPLC. J. Pharm. Biomed. Anal. 28, 903–8.

Figueroa, S.C., de Gatta, M.F., García, L.H., Hurlé, A.D.-G., Bernal, C.B., Correa, R.S., Sánchez, M.J.G., 2010. The convergence of therapeutic drug monitoring and pharmacogenetic testing to optimize efavirenz therapy. Ther. Drug Monit. 32, 579–585.

Gerschenson, M., Erhart, S.W., Paik, C.Y., St Claire, M.C., Nagashima, K., Skopets, B., Harbaugh, S.W., Harbaugh, J.W., Quan, W., Poirier, M.C., 2000. Fetal mitochondrial heart and skeletal muscle damage in Erythrocebus patas monkeys exposed in utero to 3'-azido-3'-deoxythymidine. AIDS Res. Hum. Retroviruses 16, 635–44.

Goldberg, O., Moretti, M., Levy, A., Koren, G., 2015. Exposure to nitrofurantoin during early pregnancy and congenital malformations: a systematic review and meta-analysis. J. Obstet. Gynaecol. Canada JOGC = J. d'obstétrique gynécologie du Canada JOGC 37, 150–6.

Gunness, P., Aleksa, K., Koren, G., 2011. Acyclovir is a substrate for the human breast cancer resistance protein (BCRP/ABCG2): implications for renal tubular transport and acyclovir-induced nephrotoxicity. Can. J. Physiol. Pharmacol. 89, 675–80.

Hahnova-Cygalova, L., Ceckova, M., Staud, F., 2011. Fetoprotective activity of breast cancer resistance protein (BCRP, ABCG2): expression and function throughout

pregnancy. Drug Metab. Rev. 43, 53–68.

Haines, T.H., Dencher, N.A., 2002. Cardiolipin: a proton trap for oxidative phosphorylation. FEBS Lett. 528, 35–9.

HIV/AIDS, J.U.N.P. on, 2013. Global Report|UNAIDS report on the global AIDS epidemic 2013, UNAIDS. WHO Library. doi:IBN 978-92-9253-032-7

Kalabis, G.M., Petropoulos, S., Gibb, W., Matthews, S.G., 2007. Breast cancer resistance protein (Bcrp1/Abcg2) in mouse placenta and yolk sac: ontogeny and its regulation by progesterone. Placenta 28, 1073–81.

Lee, C.A., O'Connor, M.A., Ritchie, T.K., Galetin, A., Cook, J.A., Ragueneau-Majlessi, I., Ellens, H., Feng, B., Taub, M.E., Paine, M.F., Polli, J.W., Ware, J.A., Zamek-Gliszczynski, M.J., 2015. Breast Cancer Resistance Protein (ABCG2) in Clinical Pharmacokinetics and Drug Interactions: Practical Recommendations for Clinical Victim and Perpetrator Drug-Drug Interaction Study Design. Drug Metab. Dispos. 43, 490–509.

Löscher, W., Potschka, H., 2005. Role of drug efflux transporters in the brain for drug disposition and treatment of brain diseases. Prog. Neurobiol. 76, 22–76.

Lowry, O.H., Rosebrough, N.J., Farr, A.L., Randall, R.J., 1951. Protein measurement with the Folin phenol reagent. J. Biol. Chem. 193, 265–75.

Maliepaard, M., Scheffer, G.L., Faneyte, I.F., van Gastelen, M.A., Pijnenborg, A.C.L.M., Schinkel, A.H., van de Vijver, M.J., Scheper, R.J., Schellens, J.H.M., 2001. Subcellular Localization and Distribution of the Breast Cancer Resistance Protein Transporter in Normal Human Tissues. Cancer Res. 61, 3458–3464.

Mao, Q., 2008. BCRP/ABCG2 in the placenta: expression, function and regulation. Pharm. Res. 25, 1244–55.

Marchini, T., Magnani, N., D'Annunzio, V., Tasat, D., Gelpi, R.J., Alvarez, S., Evelson, P., 2013. Impaired cardiac mitochondrial function and contractile reserve following an acute exposure to environmental particulate matter. Biochim. Biophys. Acta 1830, 2545–52.

McCann, K.A., Williams, D.W., McKee, E.E., 2012. Metabolism of deoxypyrimidines and deoxypyrimidine antiviral analogs in isolated brain mitochondria. J. Neurochem. 122, 126–37.

Mela, L., Seitz, S., 1979. Isolation of mitochondria with emphasis on heart mitochondria from small amounts of tissue. Methods Enzymol. 55, 39–46.

Meyer zu Schwabedissen, H.E., Jedlitschky, G., Gratz, M., Haenisch, S., Linnemann, K., Fusch, C., Cascorbi, I., Kroemer, H.K.,. Variable expression of MRP2 (ABCC2) in human placenta: influence of gestational age and cellular differentiation. Drug Metab. Dispos. 33, 896–904.

Meyer Zu Schwabedissen, H.E.U., Grube, M., Heydrich, B., Linnemann, K., Fusch, C., Kroemer, H.K., Jedlitschky, G.,. Expression, localization, and function of MRP5 (ABCC5), a transporter for cyclic nucleotides, in human placenta and cultured human trophoblasts: effects of gestational age and cellular differentiation. Am. J. Pathol. 166, 39–48.

Neumanova, Z., Cerveny, L., Ceckova, M., Staud, F., 2016. Role of ABCB1, ABCG2, ABCC2 and ABCC5 transporters in placental passage of zidovudine. Biopharm. Drug Dispos. 37, 28–38.

Neumanova, Z., Cerveny, L., Ceckova, M., Staud, F., 2015. Role of ABCB1, ABCG2, ABCC2 and ABCC5 transporters in placental passage of zidovudine. Biopharm. Drug Dispos.

Ni, Z., Bikadi, Z., Rosenberg, M.F., Mao, Q., 2010. Structure and function of the human breast cancer resistance protein (BCRP/ABCG2). Curr. Drug Metab. 11, 603–17.

Pacheco, S.E., McIntosh, K., Lu, M., Mofenson, L.M., Diaz, C., Foca, M., Frederick, M., Handelsman, E., Hayani, K., Shearer, W.T., Women and Infants Transmission Study, 2006. Effect of perinatal antiretroviral drug exposure on hematologic values in HIV-uninfected children: An analysis of the women and infants transmission study. J. Infect. Dis. 194, 1089–97.

Pan, G., Giri, N., Elmquist, W.F., 2007. Abcg2/Bcrp1 mediates the polarized transport of antiretroviral nucleosides abacavir and zidovudine. Drug Metab. Dispos. 35, 1165–73.

Patterson, T.A., Binienda, Z.K., Lipe, G.W., Gillam, M.P., Slikker, W.J., Sandberg, J.A., 1997. Transplacental Pharmacokinetics and Fetal Distribution of Azidothymidine, Its Glucuronide, and Phosphorylated Metabolites in Late-Term Rhesus Macaques after Maternal Infusion. Drug Metab. Dispos. 25, 453–459.

Peroni, R.N., Di Gennaro, S.S., Hocht, C., Chiappetta, D.A., Rubio, M.C., Sosnik, A., Bramuglia, G.F., 2011. Efavirenz is a substrate and in turn modulates the expression of the efflux transporter ABCG2/BCRP in the gastrointestinal tract of the rat. Biochem. Pharmacol. 82, 1227–33.

Roma, M.I., Hocht, C., Chiappetta, D.A., Di Gennaro, S.S., Minoia, J.M., Bramuglia, G.F., Rubio, M.C., Sosnik, A., Peroni, R.N., 2015. Tetronic(®) 904-containing polymeric micelles overcome the overexpression of ABCG2 in the blood-brain barrier of rats and boost the penetration of the antiretroviral efavirenz into the CNS. Nanomedicine (Lond). 10, 2325–37.

Saunders, N.R., Daneman, R., Dziegielewska, K.M., Liddelow, S.A., 2013. Transporters of the blood-brain and blood-CSF interfaces in development and in the adult. Mol.

Aspects Med. 34, 742–52.

Saunders, N.R., Liddelow, S.A., Dziegielewska, K.M., 2012. Barrier mechanisms in the developing brain. Front. Pharmacol. 3, 46.

Sibiude, J., Le Chenadec, J., Bonnet, D., Tubiana, R., Faye, A., Dollfus, C., Mandelbrot, L., Delmas, S., Lelong, N., Khoshnood, B., Warszawski, J., Blanche, S., French National Agency for Research on AIDS and Viral Hepatitis French Perinatal Cohort/Protease Inhibitor Monotherapy Evaluation Trial, 2015. In utero exposure to zidovudine and heart anomalies in the ANRS French perinatal cohort and the nested PRIMEVA randomized trial. Clin. Infect. Dis. 61, 270–80.

Staud, F., Cerveny, L., Ceckova, M., 2012. Pharmacotherapy in pregnancy; effect of ABC and SLC transporters on drug transport across the placenta and fetal drug exposure. J. Drug Target. 20, 736–63.

Szabados, E., Fischer, G.M., Toth, K., Csete, B., Nemeti, B., Trombitas, K., Habon, T., Endrei, D., Sumegi, B., 1999. Role of reactive oxygen species and poly-ADP-ribose polymerase in the development of AZT-induced cardiomyopathy in rat. Free Radic. Biol. Med. 26, 309–17.

Szewczyk, A., Wojtczak, L., 2002. Mitochondria as a Pharmacological Target. Pharmacol. Rev. 54, 101–127.

Vanasco, V., Saez, T., Magnani, N.D., Pereyra, L., Marchini, T., Corach, A., Vaccaro, M.I., Corach, D., Evelson, P., Alvarez, S., 2014. Cardiac mitochondrial biogenesis in endotoxemia is not accompanied by mitochondrial function recovery. Free Radic. Biol. Med. 77, 1–9.

Wang, H., Wu, X., Hudkins, K., Mikheev, A., Zhang, H., Gupta, A., Unadkat, J.D., Mao, Q., 2006. Expression of the breast cancer resistance protein (Bcrp1/Abcg2) in tissues

from pregnant mice: effects of pregnancy and correlations with nuclear receptors. AJP Endocrinol. Metab. 291, E1295–E1304.

Wang, X., Furukawa, T., Nitanda, T., Okamoto, M., Sugimoto, Y., Akiyama, S.-I., Baba, M., 2003. Breast cancer resistance protein (BCRP/ABCG2) induces cellular resistance to HIV-1 nucleoside reverse transcriptase inhibitors. Mol. Pharmacol. 63, 65–72.

Wang, X., Nitanda, T., Shi, M., Okamoto, M., Furukawa, T., Sugimoto, Y., Akiyama, S., Baba, M., 2004. Induction of cellular resistance to nucleoside reverse transcriptase inhibitors by the wild-type breast cancer resistance protein. Biochem. Pharmacol. 68, 1363–70.

Weiss, J., Rose, J., Storch, C.H., Ketabi-Kiyanvash, N., Sauer, A., Haefeli, W.E., Efferth, T., 2007. Modulation of human BCRP (ABCG2) activity by anti-HIV drugs. J. Antimicrob. Chemother. 59, 238–45.

Yagi, K., 1976. A simple fluorometric assay for lipoperoxide in blood plasma. Biochem. Med. 15, 212–6.

Yasuda, S., Itagaki, S., Hirano, T., Iseki, K., 2005. Expression level of ABCG2 in the placenta decreases from the mid stage to the end of gestation. Biosci. Biotechnol. Biochem. 69, 1871–6.

Yonetani, T., 1967. Oxidation and Phosphorylation, Methods in Enzymology, Methods in Enzymology. Elsevier.

Zhang, Y., Huo, M., Zhou, J., Xie, S., 2010. PKSolver: An add-in program for pharmacokinetic and pharmacodynamic data analysis in Microsoft Excel. Comput. Methods Programs Biomed. 99, 306–14.

Figures and Table legends

Figure 1. Effect of chronic AZT on the expression of ABCG2 in placenta and fetal brain

(A) Representative immunoblots for ABCG2 and actin performed in placenta (left) or fetal brain (right) at post gestational day E21 isolated from control pregnant rats or after chronic oral administration of either AZT (60 mg/kg) or vehicle (0.05% ethanol). (B) Corresponding semi quantification for control (white bars, n=3), vehicles (VEH, squared bars, n=6) or AZT (stripped bars, n=6) in placenta (left) or fetal brain (right). Data are presented as media ± S.E.M relative densitometric units calculated as ratio between optical density of ABCG2 (mouse anti-ABCG2 antibody; BXP-21 clone, 1/400) and actin (n=6 different litters for each group). Statistically significant difference (**p<0.001 for placenta; *p<0.01 for fetal brain) between AZT and either CONTROL or VEH. Histology: Representative images of H&E-stained hemi-coronal sections at the striatal level from fetal brain at E21 isolated from animals chronically exposed either to vehicle (0.5% ethanol, C) or to 60 mg/kg AZT (F), n=4 per group. The scale bar in the inset represents 1 mm, whereas the area delimited by the black box is shown amplified to 200x magnification. Immunofluorescence of ABCG2: Representative photomicrographs of 20 µm-thickness cryosections from fetal brain at E21 isolated from VEH (D, E) or AZT (G, H), n=4 per group. Photomicrographs of the striatal region are shown at 100X (D and G) and magnifications (1000X) of the boxes marked in D and G are shown (G and H, respectively).

Table 1. **Effect of chronic oral administration of AZT in mitochondrial function in fetal brain.** Oxygen consumption rates were evaluated by high-resolution respirometry in isolated mitochondria from fetal brain. 2 mM Malate plus 5 mM glutamate, or 8 mM succinate, were used as respiratory substrates to establish state 4 respiration. Afterwards, 1 mM ADP was added to archive state 3 metabolic state. RCR was calculated as state 3/state 4 respiration rates. RCR: respiratory control ratio

Table 2. Effect of chronic oral administration of AZT in mitochondrial respiratory chain complexes activity. Colorimetric assessment of mitochondrial respiratory chain complexes activity, based on cytochrome c^{3+} reduction for Complexes I and II, and on cytochrome c^{2+} oxidation for Complex IV, in mitochondrial membranes isolated from fetal brains of either vehicle (VEH, white bars) or AZT (stripped bars) treated pregnant rats in E21.

Figure 2. Evaluation of isolated brain mitochondrial membrane potential by flow cytometry.

(A) Mitochondria were selected based on light scattering properties and 20,000 gated events were collected. (B) Overlaid histograms and (C) fluorescence quantification of gated mitochondrial events for NAO, indicating purity of the mitochondrial preparations and cardiolipin oxidation. Autofluorescence (grey), control (light orange), AZT (dark orange). (D) Overlaid histograms and (E) fluorescence quantification of gated mitochondrial events for DiOC6, indicating mitochondrial inner membrane potential. Autofluorescence (grey), control (light green), AZT (dark green).

Figure 3. Effect of chronic AZT on mitochondrial ultrastructure and lipid oxidation in fetal brain.

Representative electron microscopy photomicrographs (30,000X) of fetal brain cortex at E21 after *in utero* chronic exposure to 60 mg/kg body weight AZT (F-I) or vehicle (0.05% ethanol, A-D). Boxes in B and G are shown at greater magnification (85,000X) in F and J, respectively. The photos show swelling of mitochondria (blue arrow), dissolution of some cristae (violet arrow) or light matrix (red arrow) and disruption of mitochondrial membranes (green arrow). (K) Quantification of mitochondrial damage in brain cortex from VEH (white bar) or AZT (stripped bar) groups. Ten photomicrographs per sample (n=3 per group by duplicated) were analyzed based on the followed scoring: 0- Mitochondrion with intact membrane, compact, well-defined cristae, and a dark matrix. 1- Mitochondrion with light matrix. 2- Mitochondrion with cloudy swelling. 3- Amorphous material collection inside the mitochondrion. 4- Mitochondrion membrane rupture. (L) Lipid oxidation was evaluated by the TBARS assay in fetal brain homogenates, from either vehicle (VEH, white bars) or AZT (stripped bars) treated pregnant rats in E21.

Figure 4. Effect of chronic oral administration of AZT on its pharmacokinetic in maternal blood

Kinetics of AZT in maternal blood after an i.v. administration of 60 mg AZT/kg body weight to pregnant rats at E21 after repeated oral administration of AZT (black circles) or its vehicle (VEH, open circles) from t1 to t30 min. Assays were onset after 30 min of an i.p.

administration of the ABCG2 inhibitor gefitinib (20 mg/kg body weight; GFT; B) or the corresponding vehicle (dimethyl sulfoxide:propylene glycol:saline solution, in a 2:2:1 ratio, respectively; VEH; A). Data are presented as mean ± SEM of the μg AZT/ml for each time point. (C) Area under the curve of AZT from 0 to infinite in maternal blood (AUC $AZT_{0\rightarrow\infty\ plasma}$) after repeated oral administration of AZT or its vehicle in the presence (AZT / GFT and VEH / GFT, respectively) or absence (AZT / VEH and VEH / VEH, respectively) of gefitinib. Data is presented as mean ± SEM of the μg. ml^{-1} min^{-1} of AZT for 6 animals per group.

Figure 5. Effect of chronic oral administration of AZT on its accumulation in the distribution to the fetal brain

Kinetics of AZT in fetal brain after an i.v. administration of 60 mg AZT/kg body weight to pregnant rats at E21 after repeated oral administration of AZT (black circles) or its vehicle (open circles) from t1 to t30 min. Assays were onset after 30 min of an i.p. administration of the ABCG2 inhibitor gefitinib (20 mg/kg body weight; GFT; B) or the corresponding vehicle (dimethyl sulfoxide:propylene glycol:saline solution, in a 2:2:1 ratio, respectively; VEH; A). Data are presented as mean ± SEM of the μg AZT/ml for each time point, *$p<0.05$; **$p<0.01$ between VEH / VEH and AZT / VEH for each time point in control conditions. (C) Area under the curve of AZT from 0 to infinite in fetal brain (AUC $AZT_{0\rightarrow\infty\ fetal\ brain}$) after repeated oral administration of AZT or its vehicle in the presence (AZT / GFT and VEH / GFT, respectively) or absence (AZT / VEH and VEH / VEH, respectively) of gefitinib. Data is presented as mean ± SEM of the μg. ml^{-1} min^{-1} of AZT for 6 animals per group. [a]$p<0.001$ between VEH / VEH and AZT / VEH groups; [b]$p<0.001$ between AZT /

VEH and AZT / GFT groups. (D) AUC $AZT_{0\rightarrow\infty\ fetal\ brain}$/ AUC $AZT_{0\rightarrow\infty\ plasma}$ ratio. [a]$p<0.001$ between VEH / VEH and AZT / VEH groups; [b]$p<0.001$ between AZT / VEH and AZT / GFT groups.

Supplemental File 1.

(A) Representative immunoblot for ABCG2 (72 kDa) and actin (42 kDa) performed in placenta at E11, E15, E18 or E21 (left) and fetal brains at E18 or E21 (right) from control pregnant rats. (B) Corresponding semi-quantification presented as media ± S.E.M relative densitometric units calculated as ratio between optical density of ABCG2 (polyclonal anti-rat ABCG2 antibody M-70, 1/400) and actin (n=3 pregnant rats for each gestational day). For placenta (left): a= different from E11 with $p<0.001$, b= different from E15 with $p<0.001$; for fetal brain (right): *=$p<0.01$ between E18 and E21. For details see Methods.

Figure 1

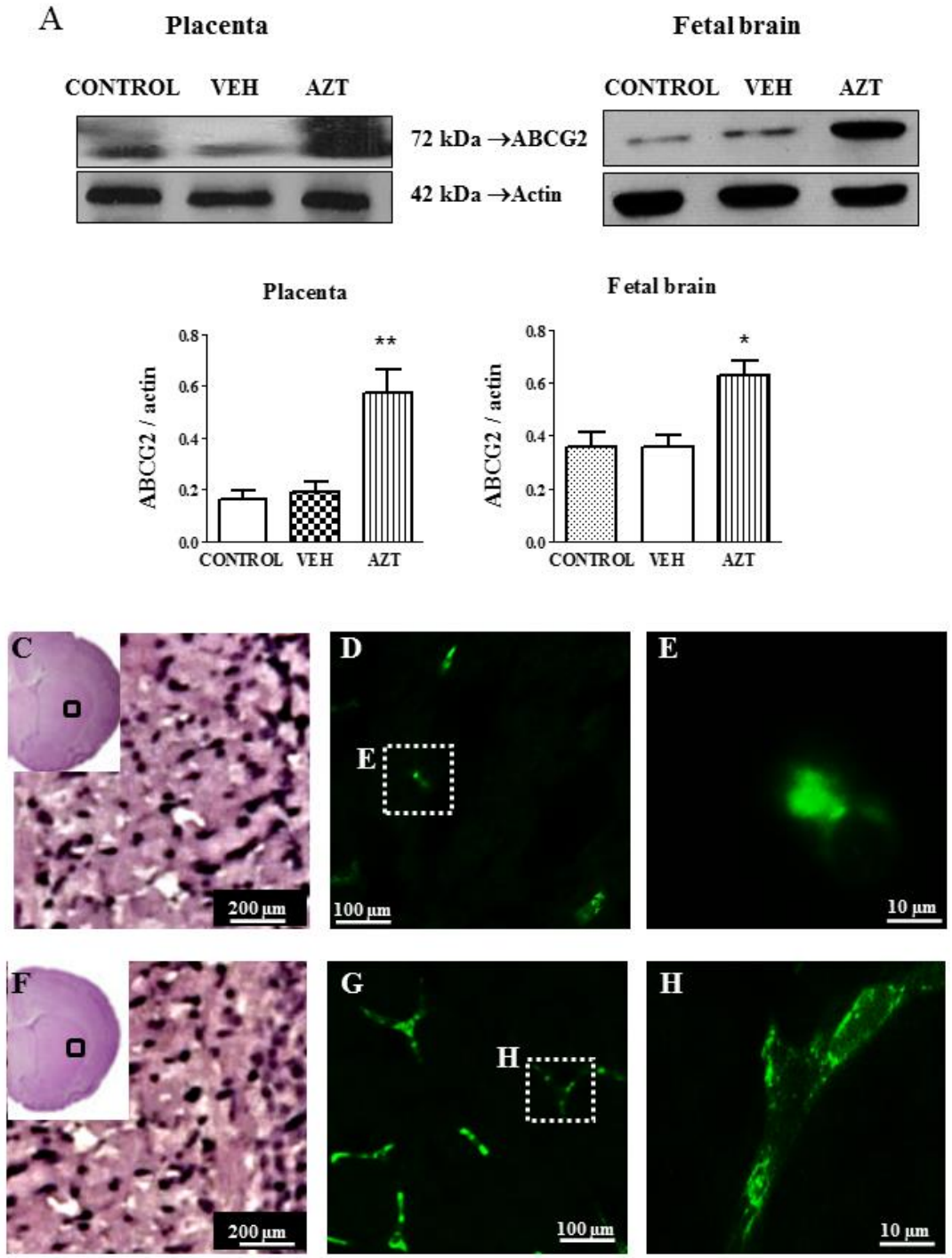

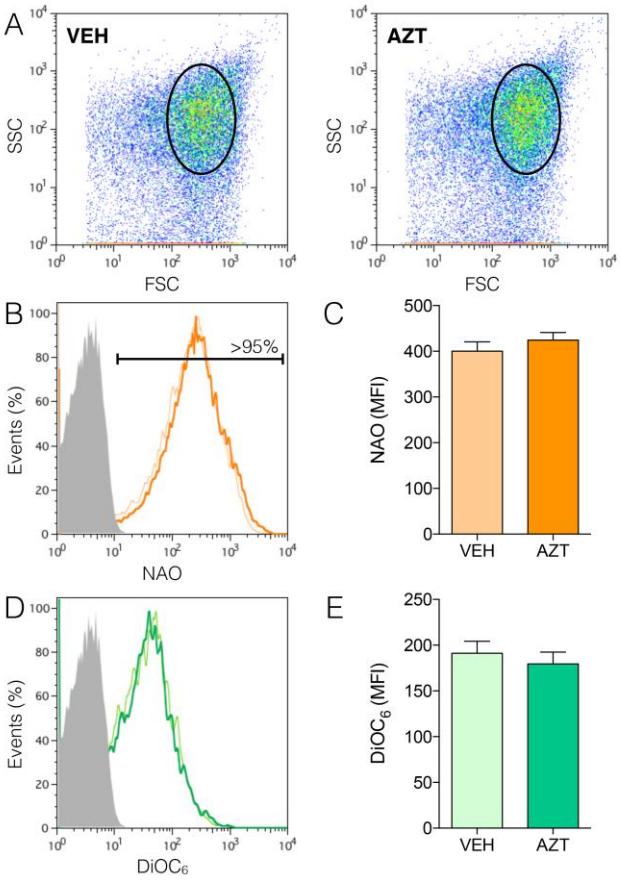

Figure 2

Figure 3

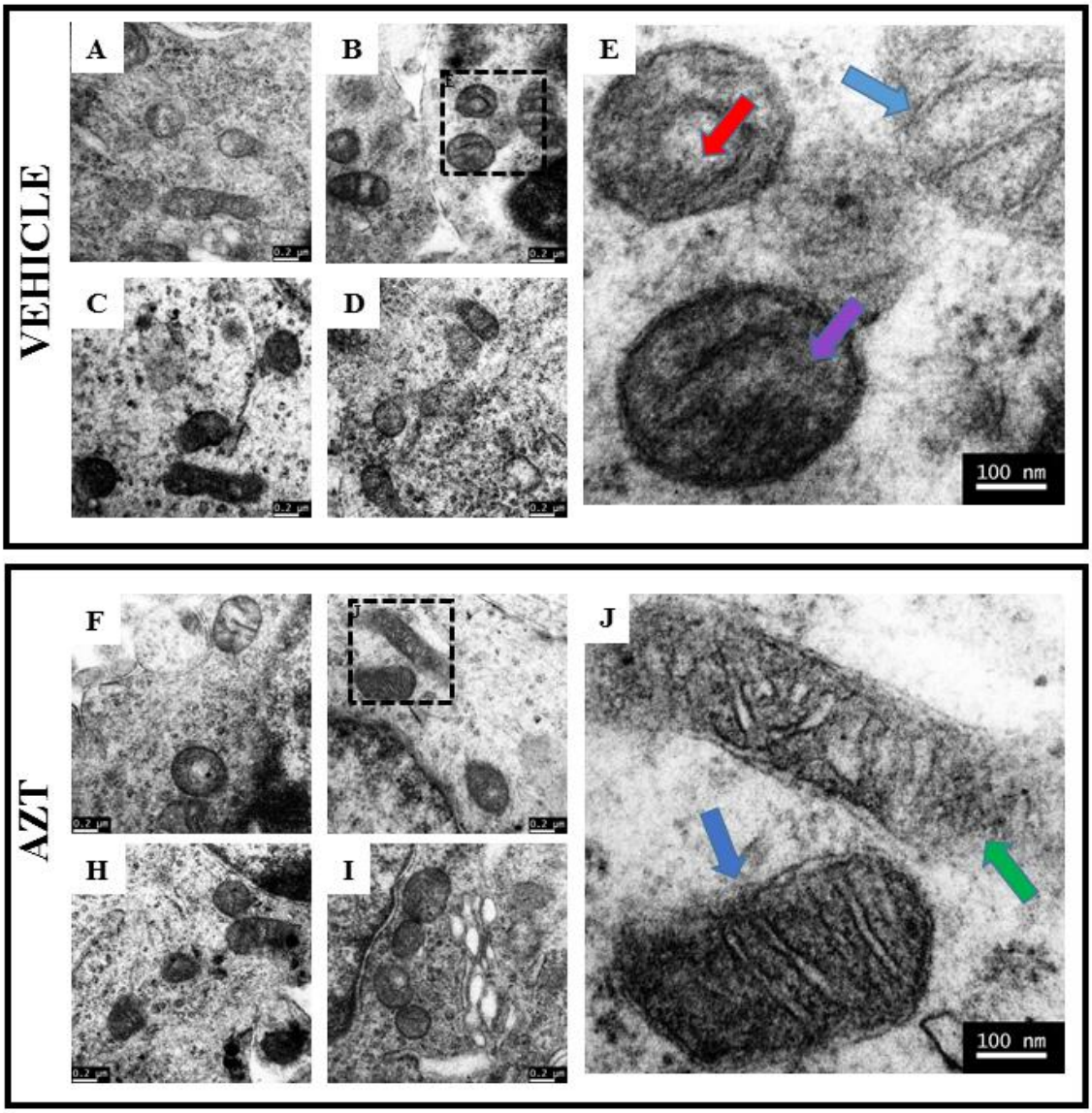

Figure 4

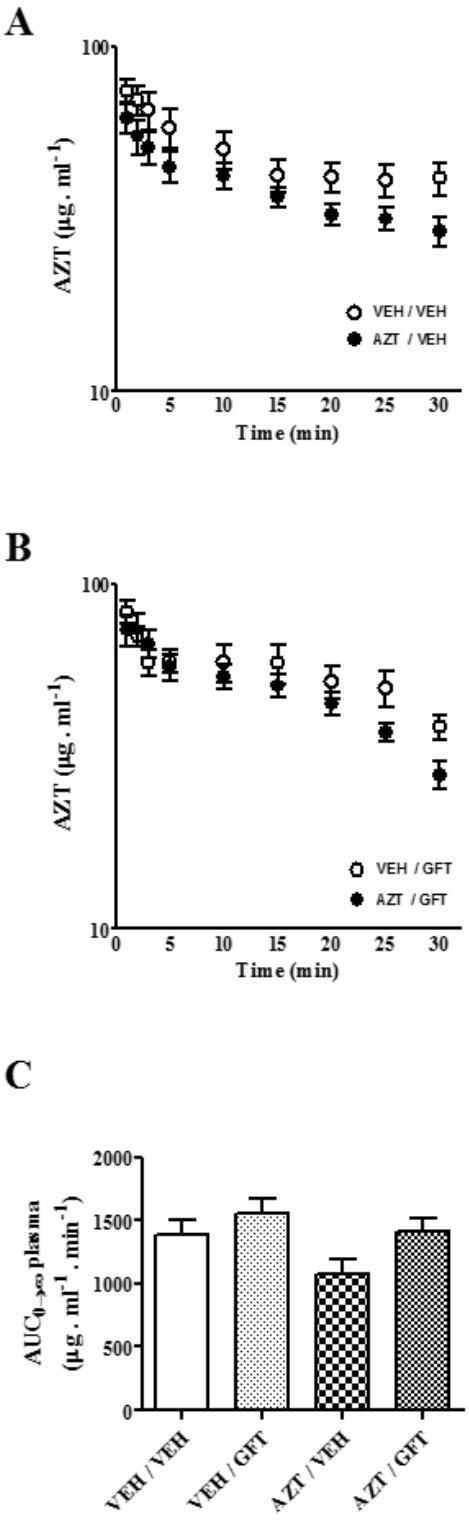

Figure 5

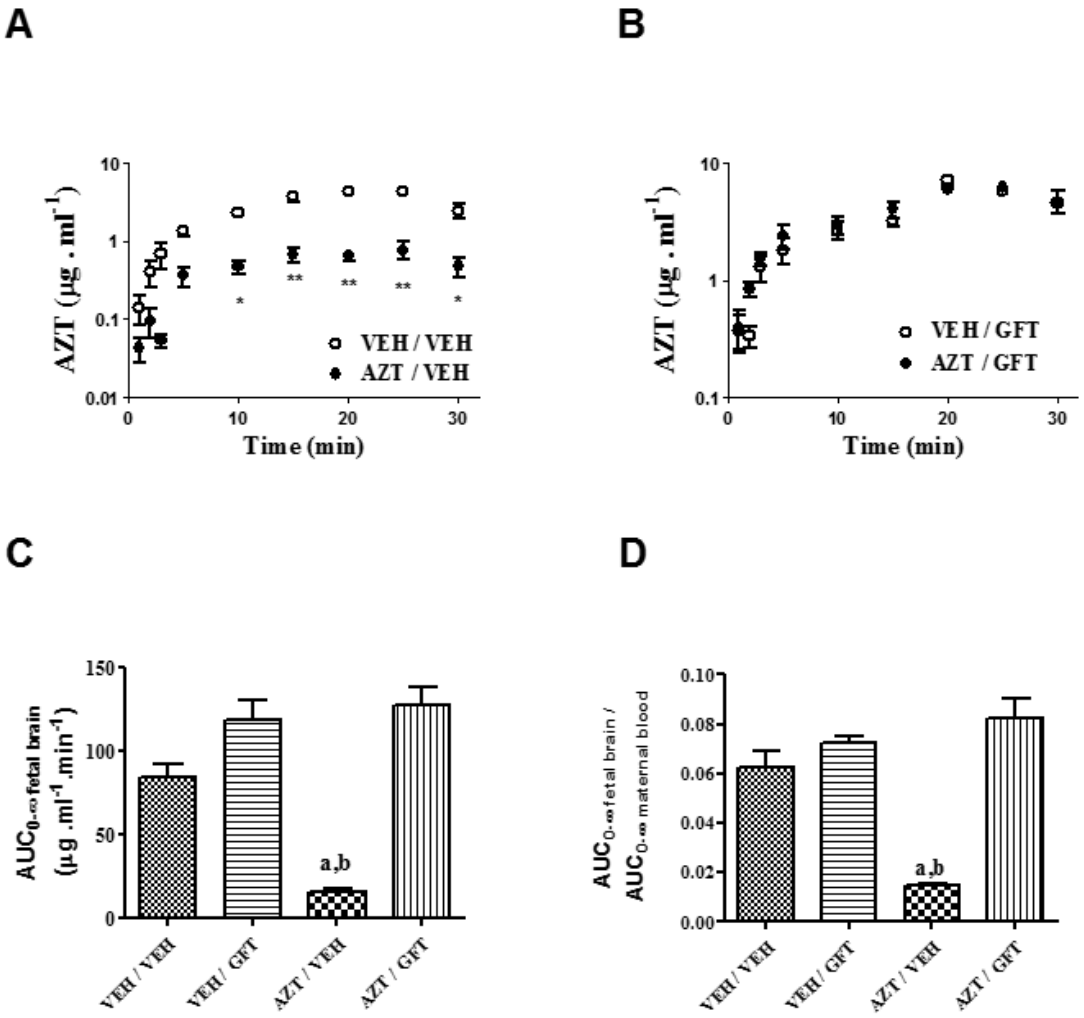

Table 1. Mitochondrial oxygen consumption

	VEH	AZT
Malate + Glutamate		
State 4	11 ± 1	13 ± 2
State 3	55 ± 4	58 ± 14
RCR	5,1	4,2
Succinate		
State 4	23 ± 4	26 ± 6
State 3	69 ± 10	71 ± 20
RCR	3,0	2,7

RCR= Respiratory control ratio

Table 2. Mitochondrial respiratory chain complexes activity.

	Complex I (nmol/min mg prot)	**Complex II (nmol/min mg prot)**	**Complex IV (k´/mg prot)**
VEH	203 ± 8	60 ± 4	113 ± 10
AZT	207 ± 13	62 ± 7	150 ± 17

Highlight

- -AZT induced the expression of ABCG2 in the placenta and the fetal brain.
- -Induction of ABCG2 restricted AZT disposition in the fetal brain.
- -Induction of ABCG2 did not modify AZT levels in maternal blood.
- -Chronic in-utero exposure to AZT did not alter mitochondria function.
- -Chronic in-utero exposure to AZT did not alter mitochondria ultrastructure.